4-2021

# Applying Machine Learning to Neutron-Gamma Ray Discrimination from Scintillator Readout Using Wavelength Shifting Fibers

Michael K. Moore CDT'21
*United States Military Academy*, michael.moore@westpoint.edu

M H. Scherrer
*Worcester Polytechnic Institute*, scherrer.m.bsb@gmail.com

Sean Clement
*Naval Postgraduate School*, sean.clement@nps.edu

Daniel S. Hawthorne
*United States Military Academy*, dshawth@pm.me

Daniel C. Ruiz
*United States Military Academy*, daniel.ruiz@westpoint.edu

## Authors

Michael K. Moore CDT'21, M H. Scherrer, Sean Clement, Daniel S. Hawthorne, Daniel C. Ruiz, Chad C. Schools, Craig Smith, and Brian Wade

Vol. 39, No. 1
April 2021

JOURNAL OF
RADIATION
EFFECTS
Research and Engineering

# Applying Machine Learning to Neutron-Gamma Ray Discrimination from Scintillator Readout Using Wavelength Shifting Fibers

M.K. Moore, M.H. Scherrer, S.A. Clement, D.S. Hawthorne, D.C. Ruiz, C.C. Schools, C.F. Smith, and B.M. Wade

This paper was accepted for presentation at the 37th Annual HEART Conference Louisville, KY, March 24–27, 2020 (Postponed); August 18–21, 2020 (Cancelled).

Prepared by Amentum for the HEART Society under contract to NSWC Crane

JOURNAL OF RADIATION EFFECTS,
Research and Engineering
Vol. 39, No. 1, April 2021

# APPLYING MACHINE LEARNING TO NEUTRON-GAMMA RAY DISCRIMINATION FROM SCINTILLATOR READOUT USING WAVELENGTH SHIFTING FIBERS

M.K. Moore
Department of Physics and Nuclear Engineering, United States Military Academy
West Point, NY

M.H. Scherrer
Department of Electrical and Computer Engineering, Worcester Polytechnic Institute
Worcester, MA

S.A. Clement and B.M. Wade
The Research and Analysis Center-Monterey, Army Futures Command
Monterey, CA

D.S. Hawthorne and D.C. Ruiz
Department of Electrical Engineering and Computer Science, United States Military Academy
West Point, NY

C.C. Schools
Nuclear Science and Engineering Research Center, Defense Threat Reduction Agency
West Point, NY

C.F. Smith
Department of Physics, Naval Postgraduate Schools
Monterey, CA

## Abstract

*Advances in machine learning have found wide applications including radiation detection. In this work, machine learning is applied to neutron-gamma ray discrimination of an organic liquid scintillator (OLS) readout using wavelength shifting (WLS) fibers. The objective of using WLS fiber is to enable the transfer of the light signal from the scintillation medium, with almost any active volume geometry, to a low-profile photomultiplier. This is a common practice in high-energy physics research and has proven to be very effective for such applications. The drawback of this approach is the light pulses carried to the photomultiplier through the WLS fibers do not perfectly replicate the original OLS light pulses' intensities or timing. This drawback causes traditional pulse shape discrimination algorithms applied to the degraded light pulses to fail to discriminate between neutron and gamma ray events. However, differences in the degraded light pulses for neutrons and gamma rays still exist and various machine learning algorithms can be applied to identify these differences. An experimental system was constructed to simultaneously capture part of the scintillation medium signal and the corresponding signal through the WLS fibers. Using the known neutron-gamma ray discrimination characteristics directly measured in the scintillation medium to provide the ground truth, supervised machine learning algorithms were applied to the corresponding light pulses carried to the photomultiplier through the WLS fibers. The results indicate that this approach will enable enhanced recovery of neutron-gamma ray discrimination information. This research effort will focus on two aspects of the OLS-WLS system: 1) developing an experimental system to create machine learning training data and 2) applying and evaluating various machine learning algorithms.*

## Introduction

The purpose of this work is to develop a fast neutron (and gamma ray) detector for security operations that is low cost and can be constructed in various geometries. For many years, helium-3 (3He)-based neutron detectors were the gold standard because of their high thermal neutron detection efficiencies and excellent neutron-gamma ray (n-γ) discrimination [1]. The cost and limited availability of 3He has made its large quantity procurement by local first responders infeasible. The proportional counter configuration of 3He detectors and the requirement for additional material to moderate incident neutrons limits the form factors of 3He-based detection systems. Organic liquid scintillator (OLS)-based fast neutron detection systems can provide low-cost solutions but are generally constrained to bulky right circular cylinder geometries to optimize light collection and n-γ discrimination. This geometry allows a greater portion of the OLS light to be incident on the photocathode of the photomultiplier tube (PMT) but limits the active volume of the detector. Wavelength shifting (WLS) fibers have been used to readout the optical signal from various plastic and liquid scintillators [1]–[9]. Reading out the OLS light signal with WLS fibers and using low-profile photomultipliers can allow more portable detection geometries to be developed with greater active detection volumes. The concept is shown in Fig. 1.

For an OLS detector readout using WLS fibers to be feasible, some level of n-γ discrimination is required.

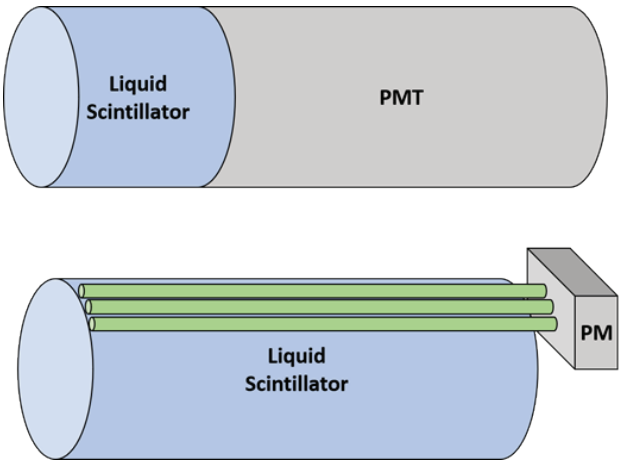


**Figure 1.** Using wavelength shifting fibers (green tubes) to readout light produced in a liquid scintillator will allow systems to be designed with more active detection volume compared to traditional right circular cylinder systems.

Traditional pulse shape discrimination (PSD) algorithms rely on the timing of scintillation light production. In our proposed system, the scintillation light from the OLS must go through the additional process of being readout using the WLS fibers. There are several steps in this process that cause distortions in the light pulses carried to the PMT through the WLS fibers. Although the distorted pulses still retain some of the original OLS pulse characteristics, traditional PSD algorithms fail to discriminate between neutrons and gamma rays. The objective of this research is to explore the potential of machine learning techniques to extract the information that remains in the distorted light pulses to discriminate between neutrons and gamma rays. This is accomplished by developing an experimental system to create training data for various supervised machine learning algorithms.

## Background

### *PSD*

In some scintillators, a larger percentage of light is produced later in time from radiation with larger linear energy transfer (LET). In the OLS used for this experiment, neutron interactions produce protons that have higher LET than the electrons produced from gamma ray interactions. Both neutron and gamma ray interactions in the scintillator produce excited singlet and triplet states, and the luminescence produced is divided into fluorescence from singlet state de-excitation and phosphorescence from triplet state de-excitation [10]. Phosphorescence yields are very low and very delayed, resulting in negligible contributions to the measured signal. But an interaction of excited triplet state molecules resulting in excited singlet state molecules, which rapidly de-excite, is believed to be the source of this increase in light output in the tail of neutron events as shown in Fig. 2 (next page). Since higher LET radiation produces higher concentrations of triplet states, more singlet states will be created from triplet state interactions, and a larger delayed fluorescence will be produced [11]. The difference is subtle, and all detectors based on this phenomenon will have a lower limit at which there is not enough light collected to correctly discriminate between neutrons and gamma rays. Traditional PSD algorithms such as Q-ratio, rise-time, and time-over threshold are used to classify events [12]. In the proposed system, scintillation light from the OLS must go through the additional process of being readout using the WLS fibers in which information about the original OLS pulse is lost.

JOURNAL OF RADIATION EFFECTS,
Research and Engineering
Vol. 39, No. 1, April 2021

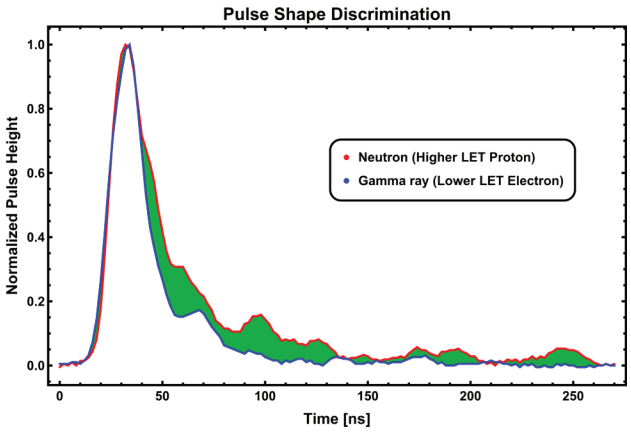


**Figure 2.** Pulse timing characteristics that is the basis of n-γ PSD. A larger percentage of light is produced later in time, shown in green, for the higher LET recoil proton from a neutron scatter than the lower LET electron from a gamma ray interaction.

### *Information Carrier Losses in the OLS-WLS System*

In a traditional scintillation detector, the photoelectrons produced as the scintillation light interacts with the photocathode are called information carriers. The quantity and timing of the photoelectrons represent all the information about the original pulse of scintillation light that is collected. To maximize the amount of scintillation light incident on the PMT's photocathode, bulky right circular cylinder containers are often used for OLS detectors. The internal surface of the containers are coated with diffuse reflecting material with high reflectance at wavelengths matching the OLS emission spectrum. As mentioned earlier, in the OLS-WLS system, the OLS scintillation light must go through the additional process of being readout using the WLS fibers.

In the proposed system, the optical photons from the OLS are converted to longer wavelength optical photons in the WLS fibers through absorption and re-emission. These WLS photons are now intermediate information carriers before they reach the photocathode and are converted to photoelectrons. Fig. 3 shows a cross-sectional view of a neutron interacting in a proposed OLS-WLS detector that has two WLS fibers attached on opposite sides of a transparent container. The neutron undergoes elastic scattering to produce a recoil proton that excites the OLS molecules as described in the previous section. An isotropic pulse of visible light emanates from along the high LET proton's path. In this system, none of these OLS photons are directly measured by a photomultiplier

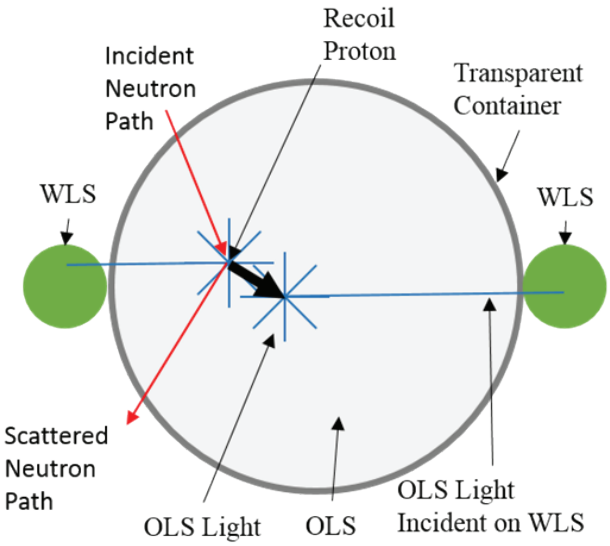


**Figure 3.** Example of a neutron interaction in an OLS-WLS system and the light losses that occur. In this example, an incident neutron undergoes scattering in the OLS, and a recoil proton is produced. The recoil proton then ionizes and excites the OLS, which isotropically produces scintillation light. A portion of the OLS light will escape the transparent OLS container and enter the WLS fibers, a portion of this light is absorbed in the WLS fibers, a portion of the absorbed light is isotropically re-emitted at longer wavelengths, a portion of the re-emitted light is emitted at an angle that will allow the light to be guided down the WLS fibers to a photomultiplier, and a portion of the light incident on the photocathode will produce photoelectrons.

and the readout process through the WLS fibers can be divided into two main steps: 1) absorption of the OLS photons in the WLS fiber material and 2) re-emission of longer wavelength WLS photons in the WLS fiber.

For an OLS photon to be absorbed, it must first enter the WLS fiber. Depending on the location of the neutron interaction in the OLS volume and the configuration of the WLS fibers around the OLS volume, there will be a geometric efficiency associated with the number of OLS photons that enter the WLS fibers. This will be further complicated by the potential for reflection, refraction, and absorption at the surfaces of the transparent OLS container and the WLS fibers. The probabilities associated with these optical photon interactions at the material boundaries have incident angle and wavelength dependency that are unknown, making the use of Monte Carlo simulations impractical. For the OLS photons that enter the WLS fibers, probability of absorption will depend on the OLS photon's wavelength (i.e., the mean free path

in the WLS material) and trajectory. The OLS emission spectrum is well matched to the WLS fiber absorption spectrum [13], [14].

The excited WLS material undergoes internal energy transfers and most of the time will radiatively de-excite emitting a photon of longer wavelength, i.e., wavelength shifted, isotropically. The de-excitation process is a random process, and various WLS materials have decay times on the order of a few nanoseconds to tens of nanoseconds. The WLS fibers act like an optical fiber and have numerical apertures dependent on shape, size, and cladding. Only wavelength-shifted photons emitted inside the numerical aperture will be internally reflected along the WLS fiber to the photomultiplier. The WLS photons that are transmitted to the end of the fiber are the intermediate information carriers and represent all the information about the original pulse of scintillation light that remains at this point in the readout process.

Finally, photoelectrons are produced as the longer wavelength WLS photons interact with the photocathode. Because the steps in this readout process are stochastic, the intensity and timing information losses are also stochastic, producing pulses that retain some of the OLS signal's shape and timing characteristics but not enough for traditional PSD algorithms to reliably distinguish between neutrons and gamma rays. Machine learning algorithms are well suited to extract these subtle and otherwise unobservable characteristics.

### *Machine Learning Algorithms*

Supervised learning is a type of machine learning that uses input data matched to known correct outputs called labels. Our first attempt to apply machine learning used an ensemble learning method and analyzed a set of data collected early in the project [15]. Promising results from this method led us to develop an improved data collection method and to apply a recurrent neural network (RNN) technique [16].

Ensemble learning consists of training multiple models and combining their outputs to achieve greater predictive power than any one model can attain. Determining the best way to combine the model outputs is a non-trivial process, and various popular methodologies range from simple averaging to more complex operations like bagging and boosting. A key aspect of training the tandem models involves ensuring they are uncorrelated, as training correlated models can often cause them to dominate other models in the ensemble and halt progress.

Additionally, we exploited the sequential nature of our data to train an RNN as our second machine learning technique. RNNs are deep neural networks that use specialized neurons to maintain an internal memory state. This internal memory allows the network to learn from the order and position of individual values within a sequence, rather than considering each value in isolation.

## Experimental Setup

In order to provide training data for machine learning techniques, a procedure to characterize every WLS pulse as originating from a neutron or gamma ray interaction in the OLS was needed. One way to achieve this would be to separately measure radiation sources that only emit gamma rays and radiations sources that only emit neutrons. There are many radiation sources that emit gamma rays without any neutrons, but neutron sources without any gamma rays are not common. In order to classify neutron and gamma ray events in a mixed neutron-gamma ray field, a proof-of-concept experiment was built to simultaneously measure light directly from the OLS and from the WLS fibers. When an interaction happens in the OLS, a portion of the isotropically emitted OLS light is directly measured by a PMT while another portion is readout through WLS fibers as described above. Fig. 4 (next page) shows an example configuration with a transparent container of OLS being readout directly with one PMT and simultaneously being readout through five WLS fibers arranged along the bottom.

Classification of neutron or gamma ray events is accomplished by applying traditional PSD algorithms to the directly readout OLS pulses. Using more WLS fibers should result in less information losses and the WLS pulses more accurately replicating the OLS pulses. More WLS fibers also increase manufacturing complexity and costs.

The OLS used for this proof-of-concept experiment was Eljen Technology's EJ309 liquid scintillator. EJ309

JOURNAL OF RADIATION EFFECTS,
Research and Engineering
Vol. 39, No. 1, April 2021

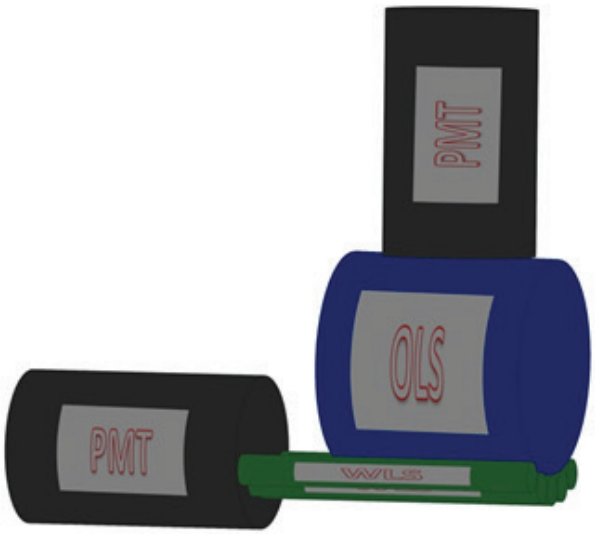


**Figure 4.** Example experimental setup to produce training data for machine learning algorithms. Light pulses produced from neutron or gamma ray events in the OLS (blue) are simultaneously readout through five WLS fibers (green) arranged along the bottom and directly through a PMT attached at the top. The light pulses measured directly from the OLS are used to classify the corresponding WLS pulses as neutron or gamma ray events.

has many desirable characteristics to include relatively low chemical toxicity, a fast decay time of 3.5 ns, a high light output of 12,300 photons/MeVee, and 5.43 x $10^{22}$ H atoms/$cm^3$ [13]. The WLS fibers used were Saint Gobain Chrystals' BCF-91A, which have an absorption spectrum that matches closely to EJ309's emission spectrum. BCF-91A's 12-ns decay time was longer than some other WLS fibers considered but with lower light attenuation [14]. The Hamamatsu R6095 PMTs were used for both the OLS light (424-nm emission peak) and the WLS fiber light (394-nm emission peak), providing similar quantum efficiency of 25% at both peak wavelengths [17]. A CAEN V1730 digitizer (14-bit, 500 MS/s) converted the analog signals from the OLS PMT and the WLS PMT [18]. Radioactive sources included gamma ray only emitters (Cs-137 and Co-60) and mixed gamma ray and neutron emitters (Cf-252 and Pu-Be). To produce experimental data for machine learning, the system was triggered on the OLS output, and both the OLS and WLS digitized pulses were saved for post-processing. Therefore, for every neutron or gamma ray pulse collected from the OLS, there is a WLS pulse that corresponds to that same neutron or gamma ray. Triggering on the OLS output ensured the majority of pulses captured could be accurately identified as neutron or gamma ray events using standard PSD methods. Data were collected using configurations with one fiber, three fibers, and six fibers to determine if applying machine learning algorithms has the potential to reduce the number of fibers required and allow for the development of less expensive detection systems.

## Machine Learning Training Data

To create the machine learning training data—i.e., a classification as neutron or gamma ray for every WLS pulse—the traditional PSD Q-ratio method was applied to the OLS pulses. The Q-ratio method uses two time-gated integrals, the total pulse ($Q_{long}$) and the fast component ($Q_{short}$), to quantify the portion of light produced in the tail of the pulse.

$$Q_{ratio} = \frac{Q_{long} - Q_{short}}{Q_{long}} \quad (1)$$

Larger $Q_{ratio}$ values correspond to neutron events. The performance of this method is sensitive to the time-gate parameters and must be optimized. A standard figure-of-merit (FOM) for PSD algorithms is used to quantify performance on the algorithm's ability to discriminate between neutron and gamma ray events [12]. Graphically shown in Fig. 5, the FOM was calculated by dividing the distance

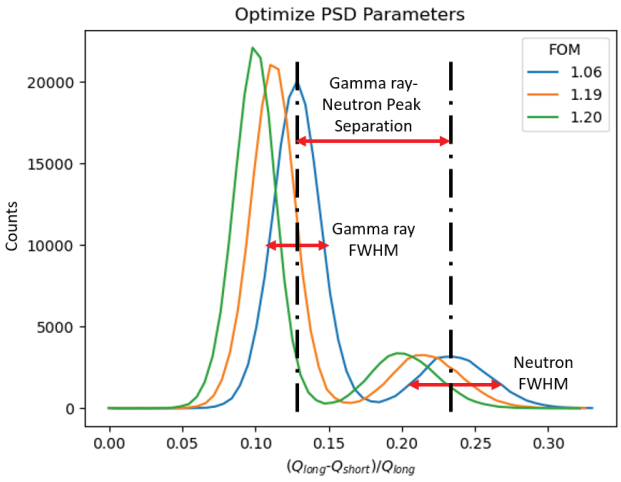


**Figure 5.** Training data are produced following optimization of the PSD Q-ratio method applied to the OLS pulses. The FOM quantifies an algorithm's ability to distinguish between neutron and gamma ray events. Greater discrimination—i.e., larger FOM value—is achieved with narrower neutron and gamma ray peaks with larger separation between the respective peaks. Time-gate values that provide the highest FOM are used to classify each event as a neutron or gamma ray.

between the gamma ray and neutron peaks, known as separation, by the sum of each peak's respective full width half maximum (FWHM). The equation for calculating the FOM is shown below.

$$FOM = \frac{Separation}{Gamma\ FWHM + Neutron\ FWHM} \quad (2)$$

We used Python 3 to develop an optimization algorithm that provided the best PSD performance using the Q-ratio method. Our solution takes the OLS pulses in their text-based format from the Caen WaveDump software [19]. The process begins by parsing the text files and storing the values in a NumPy structure [20]. The NumPy structure is very efficient and performs very well for our use-case. It allows us to operate on every value in a field when required and allocates storage for the results in advance. It also acts like an associative array, allowing key-value pairs for fields including timestamps, pulse baselines, peak values, noise within the pulse, and the $Q_{ratio}$ of a pulse. The structure includes a sub-array containing the analog-to-digital converted (ADC) values for each pulse.

Because our baseline reading fluctuated between +/- 30 on our 14-bit digitizer reading, we needed to apply an initial filter to reduce the noise prior to the application of any PSD methods. We applied a bandpass filter to the ADC values for each pulse where ADC values between the two thresholds are set to zero. This technique reduces the noise inherent to the PMT in order to improve the signal-to-noise ratio. The resulting filtered data allow us to eliminate the need to iterate over $Q_{short}$ as the lead in noise and measurement inconsistencies were mitigated by the filter. Instead of iterating over both $Q_{long}$ and $Q_{short}$, we iterated over just $Q_{long}$.

After the filter is applied, the implementation calculates the $Q_{ratio}$ for every event. To optimize the FOM, the program iterates through multiple time-gate values for $Q_{long}$ and chooses the value that will produce the largest FOM. The results of one such optimization process is shown in Fig. 5.

Once the best time-gate values are selected, the pulses are classified as neutrons if its $Q_{ratio}$ falls to the right of the minimum point between the two peaks and as gamma rays if it falls to the left of the minimum point between the two peaks. The program analyzes 100,000 events in less than 10 seconds and produces the training data that are used by the machine learning algorithms.

## Applying Machine Learning

### *Ensemble Learning Method*

Our initial application of machine learning used an ensemble learning method. The data were collected in an early version of the experimental setup but resulted in the same type of training data with each WLS pulse classified as a neutron or gamma ray based on the corresponding OLS pulse. The training data included 8062 gamma ray and 5554 neutron events from a Pu-Be source and 7705 gamma ray events from a Co-60 source.

An example of the digitized signals for both a gamma ray and neutron event is shown in Fig. 6. As can be seen in this figure, differences in wave shape exist between the neutron and gamma ray events. Six of these key differences, called features, were extracted from every training example: the minimum and maximum of each pulse, the width of the largest peak, the second minimum, the width of the second minimum, and the total area under the main impulse. These features were used to train the supervised learning models to then predict the type of radiation that was detected.

The initial training data had more gamma ray events than neutron events, which can cause bias problems

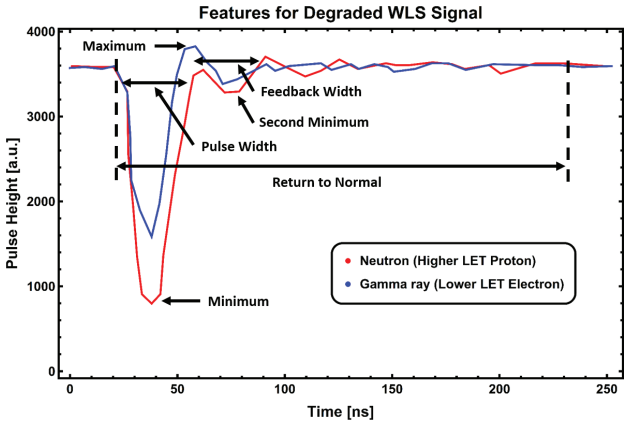


**Figure 6.** Feature engineering based on the difference between the average WLS neutron or gamma ray event. While both events may have extremely similar Q-ratios or rise times, they have distinguishable wave shapes that can be exploited to correctly predict their type.

when training machine learning algorithms. To fix this imbalance, a number of synthetic neutron events were created. This was done by taking a random sample for each time step (from 1 to 136 steps) from the neutron training dataset. Then, to dampen the variance induced by this sampling, a rolling average with a window of five time steps was used to smooth out the simulated data.

Supervised learning methods tend to over fit the data and fail to generalize to new data. To prevent this, the original and synthetic datasets were divided into training, validation, and test datasets by randomly selecting 20% of the data for the validation set and 20% of the data for the test set. The remaining 60% of the data was the training set.

The supervised learning models used in the classification task were Logistic Regression, Naive Bayes Classification, Random Forests, Support Vector Machines, Boosted Forests, and K-Nearest Neighbors Classification [21]. After the initial training and evaluation of each algorithm with 10-fold cross-validation using only the training dataset, an ensemble model was constructed using a linear combination of the above-listed models. Because the algorithm outputs were relatively uncorrelated, it was possible to combine all the models in such a way to increase the accuracy of our classifications beyond that of any one component model. Since the component models were trained on the training set, the weights for the linear coefficients of the ensemble model were found using the validation set to prevent overfitting.

This ensemble model was then exposed to the test set data. This is data that had been held out during the training and validation process, so the models had not seen the data before. On this final test set, the model correctly identified the type of radiation event 89.4% of the time. Of particular interest, the false-positive rate, where the model classified an event as neutron erroneously, was 9%. This means that when the ensemble model indicated a neutron event, the model was correct 91% of the time. The false-negative event, events where the gamma ray was indicated but the event was in truth a neutron event, occurred 12% of the time the model indicated gamma ray. This encouraging performance resulted in an improved experimental setup and the application of the RNN method.

***RNN Method***

Due to the intricacy of designing an ensemble model and the complexity required to fine-tune for future datasets, we decided to also apply an alternative machine learning approach to the problem. We began by noting the data produced from our experiments are inherently sequential, meaning the positions of ADC values within a given pulse's sequence are relevant. Given this fact, we focused our attention on RNNs as a potentially effective solution.

The training datasets were collected using Cf-252, a spontaneous fission source that emits both neutrons and gamma rays. The datasets included various WLS fiber configurations with each dataset having over 100,000 events. Our baseline model consisted of four hidden layers, each containing eight gated recurrent units (GRUs) and an output layer consisting of a single neuron with a sigmoid activation for binary classification (Fig. 7). In total, this network configuration contained approximately 500 trainable parameters, which we estimated would result in efficient training while still giving the network the ability to generalize.

GRUs are a type of recurrent neuron that enable the network to carry over information from prior elements of a sequence [22]. While often less capable than the more popular long short-term memory (LSTM) cells [23], we found the performance of GRUs to be comparable to that of LSTMs on our data and considerably faster to train. Like the ensemble implementation, we trained our baseline GRU network on 60% of available data, with the remaining 40% split evenly for validation and test sets. Two of our models utilized a technique in which the network learning rate was reduced by a fixed amount

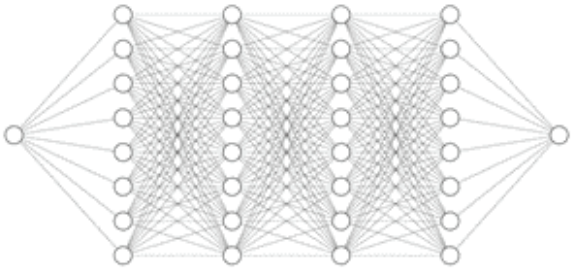

**Figure 7.** Baseline recurrent neural network architecture. Four hidden layers are each comprised of eight GRU cells with hyperbolic tangent activation functions. The final layer consists of a single neuron with a sigmoid activation to provide binary classification between neutron and gamma ray events. This architecture contains approximately 500 trainable parameters.

when accuracy started to plateau (referred to as RLRoP in Table 1, Reduce Learning Rate on Plateau). This assisted the networks in avoiding local minima while training and led to slightly higher accuracies. Using the six WLS fibers dataset, our baseline model achieved a promising 85.6% accuracy when evaluated against the entire dataset. More significantly, our baseline model was able to generalize to collections made with fewer numbers of WLS fibers. In the case of the one WLS fiber configuration, our model's predictive accuracy only suffered by a margin of 3%. (See Table 1 for all results.)

**Table 1.** Despite iterative adjustments to our architecture and hyperparameters, little improvement was made to predictive accuracy. However, the model's ability to achieve over 80% accuracy when trained on 1-fiber WLS data is promising and warrants further optimization.

| WLS Fiber Configuration | Model 1 *4xGRU(8)* | | Model 2 *4xGRU(8), RLRoP* | | Model 3 *2xGRU(128), RLRoP* | |
|---|---|---|---|---|---|---|
| | Loss | Accuracy | Loss | Accuracy | Loss | Accuracy |
| 6 WLS Fibers | 0.3441 | 85.5% | 0.3374 | 86.1% | 0.3212 | 86.8% |
| 3 WLS Fibers | 0.3629 | 85.1% | 0.3456 | 85.6% | 0.3602 | 85.6% |
| 1 WLS Fiber | 0.4357 | 82.8% | 0.4156 | 83.0% | 0.4398 | 82.6% |

As evidenced above, we continued to improve our baseline model's performance by conducting iterative hyperparameter tuning. Our best-performing model (Model 3), opted to use two fewer hidden layers in exchange for 128 GRUs in each layer. We also implemented early stopping to counteract some minimal overfitting and reduced the learning rate if a plateau was detected every 10 epochs. Despite these changes, improvements were minimal across the board, suggesting we had found a local maximum or better performance was simply not possible with a recurrent neural network approach. To further reinforce our results, we trained a new model using an identical architecture as Model 3 above, but this time using 60% of the one WLS fiber dataset as training data. This new model achieved a comparable 83.6% test accuracy.

Several conclusions can be derived from our experimentation with RNNs. First, our results were comparable to those achieved by the ensemble model with significantly less complexity and training time. More importantly, our neural network required zero feature engineering and was trained exclusively on collected ADC sequences that were pre-processed with a bandpass filter and normalized. This suggests the neural network approach may be more conducive to fast prototyping and testing of models for experimentation onboard a deployable sensor.

## Conclusion

There continues to be a need for advanced radiation detection systems intended for nuclear security operations. These systems need to be portable, have adaptable geometries, demonstrate good n-γ discrimination, and be affordable. This research provided an assessment of applying machine learning to n-γ discrimination in OLS-WLS-based fast neutron detection systems. Using Python 3, we developed an efficient way to produce training data for supervised machine learning algorithms. Machine learning using the ensemble method and the neural networks method achieved comparable and promising results and continued research in this area is warranted.

## Future Work

There remain several avenues for improvement in the machine learning algorithm. There are additional preprocessing steps that can be implemented to continue reducing the noise in our ADC sequences. Specifically, reducing the length of the data sequences may help the network focus on the important values relevant to the discrimination task. Combining datasets will expose the network to additional data and potentially improve its ability to generalize. An exploration of the application of other neural network paradigms to this problem will help with performance and accuracy. These will include one-dimensional convolutional neural networks and attention networks, the latter of which has achieved state-of-the-art results in many machine learning tasks featuring sequenced data [24].

## References

[1] Kouzes *et al.*, "Progress in alternative neutron detection to address the helium-3 shortage," *Nucl. Instruments and Methods in Physics Res. Section A: Accelerators, Spectrometers, Detectors and Associated Equipment*, vol. 784, pp. 172–175, June 2015.

[2] L. Benussi *et al.*, "Large liquid-scintillator trackers for neutrino experiments," *Nucl. Instruments and Methods in Physics Res. Section A: Accelerators, Spectrometers, Detectors and Associated Equipment*, vol. 488, no. 3, pp. 503–516, Aug. 2002.

[3] P. Border *et al.*, "A large liquid scintillator detector for a long baseline neutrino oscillation experiment," *Nucl. Instruments and Methods in Physics Res. Section A: Accelerators, Spectrometers, Detectors and Associated Equipment*, vol. 463, no. 1–2, pp. 194–204, May 2001.

[4] W. Bugg, Y. Efremenko, and S. Vasilyev, "Large plastic scintillator panels with WLS fiber readout; optimization of components," ArXiv e-prints, 1312, [Online]. Available: http://adsabs.harvard.edu/abs/2013arXiv1312.0997B. [Accessed 01 Dec. 2013].

[5] M. David, A. Gomes, A. Maio, and M. Varanda, "Optical properties of fibres for the 1998 Module 0," *ATLAS Internal Note*, vol. 98, no. 162, p. 6, 31 July 1998.

[6] M. Doucet, J.P. Fabre, G. Grégoire, J. Panman, and P. Zucchelli, "A liquid scintillator detector with wavelength-shifting fibre readout," *Nucl. Instruments and Methods in Physics Res. Section A: Accelerators, Spectrometers, Detectors and Associated Equipment*, vol. 453, no. 3, pp. 545–552, 2000.

[7] M. Doucet, J.P. Fabre, G. Grégoire, J. Panman, and P. Zucchelli, "Light yield measurements in a liquid scintillator detector with wavelength-shifting fibre readout," *Nucl. Instruments and Methods in Physics Res. Section A: Accelerators, Spectrometers, Detectors and Associated Equipment*, vol. 459, no. 3, pp. 459–468, 2001.

[8] P.L. Hink, R.E. Rothschild, M.R. Pelling, D.R. MacDonald, and D.E. Gruber, "UCSD high-energy x-ray timing experiment cosmic ray particle anticoincidence detector," *Proc. SPIE 1549, EUV, X-ray, and Gamma-Ray Instrumentation for Astronomy II*, 1 Oct. 1991.

[9] T. Nakamura *et al.*, "A scintillator-based detector with sub-100-μm spatial resolution comprising a fibre-optic taper with wavelength-shifting fibre readout for time-of-flight neutron imaging," *Nucl. Instruments and Methods in Physics Res. Section A: Accelerators, Spectrometers, Detectors and Associated Equipment*, vol. 737, pp. 176–183, 11 Feb. 2014.

[10] G.F. Knoll, *Radiation Detection and Measurement*, New York: John Wiley & Sons, 2000.

[11] G. Laustriat, "The luminescence decay of organic scintillators," *Molecular Crystals*, vol. 4, no. 1–4, pp. 127–145, 1968.

[12] P.J. Sellin, G. Jaffar, and S.D. Jastaniah, "Performance of digital algorithms for n/gamma pulse shape discrimination using a liquid scintillation detector," presented at the *2003 IEEE Nucl. Sci. Symp. Conf. Record*, 2004.

[13] "Neutron/gamma PSD liquid scintillator EJ-301, EJ-309," ELJEN Technologies, Sweetwater, TX.

[14] "Scintillation products: Scintillating optical fibers," Saint-Gobain Chrystals, Hiram, OH, 2011.

[15] R. Polikar, "Ensemble Learning," in *Ensemble Machine Learning*, Eds. C. Zhang and Y. Ma, Boston, MA: Springer, 2012, pp. 1–34.

[16] J.T. Connor, R.D. Martin, and L.E. Atlas, "Recurrent neural networks and robust time series prediction," *IEEE Trans. Neural Networks*, vol. 5, no. 2, pp. 240–254, Mar. 1994.

[17] "Hamamatsu photomultiplier tubes R6094, R6095," Hamamatsu Photonics K.K., Shimokanzo, Japan: Hamamatsu, 1996.

[18] "V1730 / V1730S - 16/8 channel 14 bit 500 MS/s digitizer - CAEN - tools for discovery," CAEN. [Online]. Available: https://www.caen.it/products/v1730/

[19] "CAEN wavedump - CAEN digitizer readout application - CAEN - tools for discovery," CAEN. [Online]. Available: https://www.caen.it/products/caen-wavedump/

[20] T.E. Oliphant, *Guide to NumPy*, 2006. [Online]. Available: https://archive.org/download/NumPyBook/NumPyBook.pdf

[21] F. Chollet, *Deep Learning with Python*, Shelter Island, NY: Manning Publications Co., 2018.

[22] T. Hastie, R. Tibshirani, and J. Friedman, *The Elements of Statistical Learning Data Mining, Inference, and Prediction*, Springer Series in Statistics (2nd ed.), New York, NY: Springer, 2009.

[23] S. Hochreiter and J. Schmidhuber, "Long short-term memory," *Neural Computation*, vol. 9, no. 8, pp. 1735–1780, 15 Nov. 1997. [Online]. Available: https://doi.org/10.1162/neco.1997.9.8.1735

[24] I. Tenney, D. Das, and E. Pavlick, "BERT rediscovers the classical NLP pipeline," arXiv preprint arXiv:1905.05950, 2019. [Online]. Available: https://www.arxiv-vanity.com/papers/1905.05950/